XIV. ENERGY CONVERSION RESEARCH*

A. Power Systems with Liquid-Metal Generators

Academic and Research Staff

Prof. G. A. Brown
Prof. E. S. Pierson

Graduate Students

E. K. Levy
R. J. Thome

1. MAGNETOHYDRODYNAMIC POWER GENERATION FOR NUCLEAR-POWERED SEA-GOING VESSELS

Introduction

An initial feasibility study has been conducted to determine whether the advantages offered by an MHD conversion system for marine use are worth further investigations.[1] In this investigation a gas Brayton MHD cycle and one example of a liquid-metal Rankine MHD cycle were used; required were a power output of 11 megawatts and a given nuclear reactor capable of transmitting a temperautre of 1500°K to the cooling fluid. This report describes these analyses briefly and gives the results.

Brayton Cycle MHD Power System

A theoretical investigation of the Brayton gas cycle was performed, with the working fluid of the MHD generator utilized as the reactor coolant, as illustrated in Fig. XIV-1

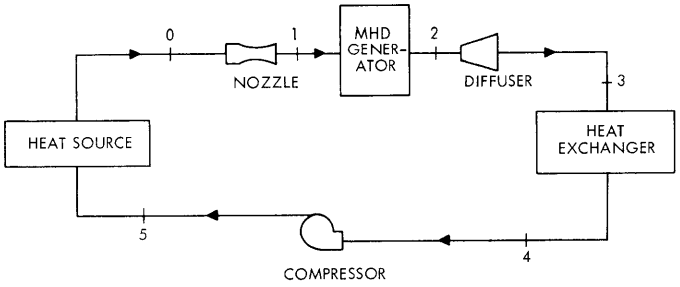

Fig. XIV-1. Brayton cycle MHD power generation system.

*This work was supported by the U. S. Air Force (Research and Technology Division) under Contract AF33(615)-3489 with the Air Force Aero Propulsion Laboratory, Wright-Patterson Air Force Base, Ohio.

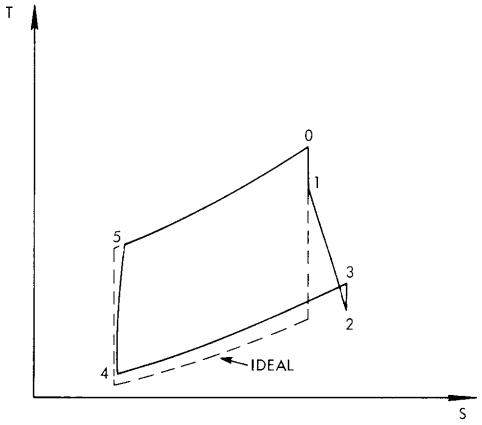

Fig. XIV-2. Diagram for the MHD Brayton cycle.

with its corresponding thermodynamic states diagrammed in Fig. XIV-2. The fluid undergoes isentropic expansion through the nozzle before the adiabatic extraction of energy in the MHD generator. The fluid is then diffused, transforming a large part of the remaining dynamic head to static pressure head, passed through a cooling heat exchanger, and finally returned to the heat source by means of an adiabatic compression process.

To provide the necessary electrical conductivity (for satisfactory operation of the MHD generator), the working fluid is seeded with a a very small percentage of an easily ionizable material (cesium, potassium) and then subjected to an extra thermal ionization process. In selecting a working fluid, one must choose one that is capable of withstanding this treatment and still maintaining satisfactory heat-transfer characteristics. Added to these restrictions, the fluid must be available, be compatible with the nuclear reactor, and have thermal conductivity qualities that take into account the volumetric limitations of ships. As a result, we found that the gas that best suited these features at the temperatures and pressures considered was helium seeded with either cesium or potassium.

Utilizing this working fluid, we conducted thermodynamic cycle analyses under the assumption of an available reactor temperature of 1500°K and with a power requirement of 11 megawatts. Significant results are cycle efficiencies of approximately 20 per cent and magnetic field requirements of approximately 40 kilogauss. This efficiency is comparable with present steam turbine systems, but the large magnetic field indicates the need for superconducting magnets. The refrigeration requirements for this magnet were not included in the study, and it is feared that the power which would be necessary to support this would reduce the over-all efficiency below acceptable levels. Furthermore, the required electrical conductivity of the working fluid (~600 mhos/m) may be higher than is practicable under current ionization methods; this would result in an even higher magnetic field in the MHD generator. Thus, futher investigation of these problem areas is needed before a substantial conclusion can be reached concerning the future use of this MHD cycle.

Rankine Cycle MHD Power System

Recent interest in liquid-metal MHD power cycles has resulted in several proposed Rankine cycles utilizing an MHD generator to convert from mechanical to electrical energy. One of these systems, the one-component, two-phase MHD cycle proposed by

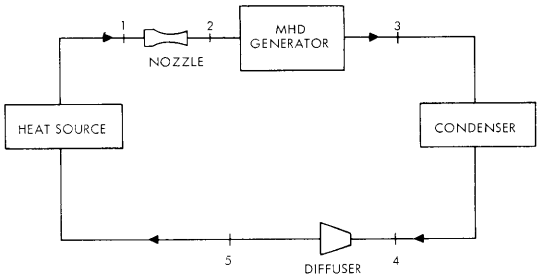

Fig. XIV-3. One-component, two-phase MHD Rankine power cycle,

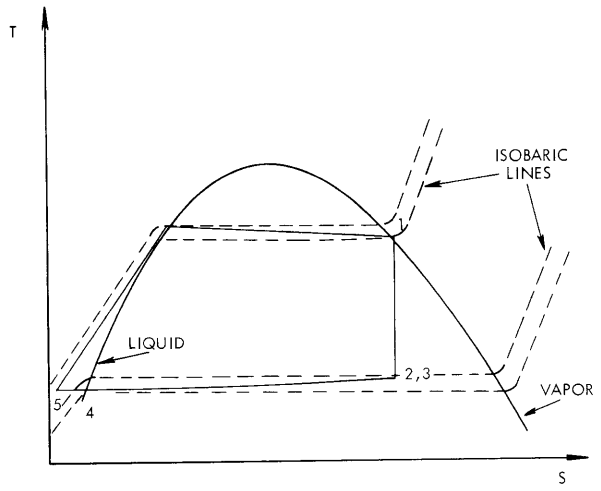

Fig. XIV-4. Thermodynamic state diagram for MHD Rankine cycle.

Petrick and Lee,[2] was chosen to typify a Rankine cycle analysis, and is schematically illustrated in Fig. XIV-3, and the thermodynamic diagram is shown in Fig. XIV-4. It is not felt that this cycle is necessarily better than other suggested liquid-metal MHD power cycles, but it was analyzed as an example of an MHD Rankine cycle. In this system, a two-phase mixture leaves the reactor heat source as a saturated vapor and increases its kinetic energy through the nozzle. The mixture then passes through the MHD generator (still in its two-phase state) where the electrical energy is removed, and into the condenser where the fluid is condensed into its liquid state and returned to the reactor by means of a diffuser.

Because the fluid in the MHD generator turns out to be a two-phase flow, about which little is known, hearty assumptions concerning its electrical conductivity were necessary to complete the cycle. It is noteworthy here to mention that with other liquid-metal MHD power cycles proposed by Elliott,[3] and by Jackson and Brown,[4] we are not faced with the particular problem of two-phase flow in the MHD generator, although they do involve troublesome components that are unnecessary in the one-component, two-phase MHD cycle. Since all of the liquid-metal cycles are still under intensive experimentation, it is not fair to pick any of them as superior at this early stage of development, but rather to bear in mind the particular advantages and complications of each.

Keeping this in mind, we conducted cycle analyses on the one-component, two-phase system, utilizing mercury and potassium as the working fluids. Significant results indicate that the thermodynamic cycle efficiency increases with the fluid's mixture quality in the generator, but the electrical conductivity of the two-phase mixture decreases markedly with increasing mixture quality, and thus the cycle may become impractical at the competitive thermodynamic efficiencies. Mercury showed a higher

efficiency than potassium (maximum mercury, 29 per cent; maximum potassium, 22 per cent), but the working pressures of mercury were extremely high (~3000 psi) which would militate against its use on a marine vessel. Both fluids resulted in abnormally low DC terminal voltages (~30 volts) and hence required the use of large current busses – an item that needs to be resolved if future use is anticipated.

An advantage of a Rankine MHD cycle is its capability to generate AC power (through the use of an MHD induction generator), as well as low-voltage DC power. This induction MHD generator, limited to liquid-metal flows, could be wound for usable voltages at suitable frequencies (i.e., 60 cps).[5] The problem still remains, however, for the induction generator, as well as for the DC conduction generation, of including the effects of all loss mechanisms and simultaneously matching the generator to the thermodynamic cycle.

Usefulness as a Marine Power Source

Because steam turbine systems on ships are inherently noisy, it is felt that the MHD conversion scheme, which utilizes electric motors, would greatly resolve this undesirable feature, with the gas Brayton cycle believed to be somewhat quieter than any of the proposed liquid-metal Rankine cycles. Because higher temperatures are now available (and required) for the MHD cycles, the systems must contain materials to obviate this problem and the associated fluid-reaction problem. These materials problems are still unsolved, although giant strides have been made in this direction, and there is no reason to believe that future developments in this field will not overcome this present restraint. Because future effective development of the steam cycle seems unlikely, while the MHD cycle is just beginning to open up new avenues for investigation there is now no strong reason to believe that future MHD systems will not far surpass in efficiency the present steam turbine systems. In conclusion, we suggest that the possibility that this type of power generation will eventually replace the steam turbine system is high, and now is the time to initiate further studies aimed at achieving more practical results than are now possible.

J. D. Hutchinson, E. S. Pierson

References

1. J. D. Hutchinson, "Magnetohydrodynamic Power Generation for Nuclear-Powered Sea-Going vessels," NAV. E. Thesis, Department of Naval Architecture and Marine Engineering, M. I. T., June 1966.
2. M. Petrick and K. Y. Lee, "Performance Characteristics of a Liquid-Metal MHD Generator," ANL-6870, Argonne National Laboratory, Argonne, Illinois, July 1964.
3. D. G. Elliott, "Two-Fluid Magnetohydrodynamic Cycle for Nuclear-Electronic Power Conversion," Am. Rocket Soc. J. 32, 6(1962).

4. W. D. Jackson and G. A. Brown, "Liquid-Metal Magnetohydrodynamic Power Generator Utilizing the Condensing Ejector," Patent Disclosure, M. I. T., Cambridge, Mass., October 1961.

5. E. S. Pierson, "The MHD Induction Machine," ScD. Thesis, Department of Electrical Engineering, M. I. T., September 1964; also AFAPL-TR-65-107, May 1966.

2. INTERACTION OF A SINGLE SPHERE OR CYLINDER WITH TRAVELING MAGNETIC FIELD

As a first step in the study of the mist flow MHD induction machine, the interaction between a rigid conducting sphere and a traveling magnetic field is considered.

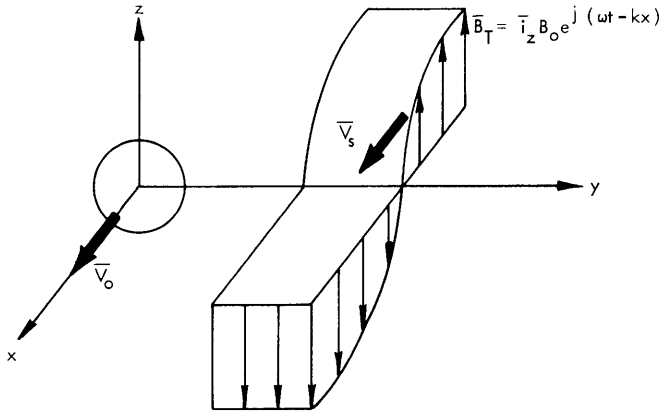

Fig. XIV-5. Configuration for sphere-field interaction.

Specifically, the configuration consists of a sphere traveling with the constant velocity $\bar{V}_o = \bar{i}_x V_o$ in an applied magnetic field with the component $\bar{B}_T = \bar{i}_z B_o e^{j(\omega t - kx)}$ transverse to the direction of motion of the sphere as shown in Fig. XIV-5. Here, ω is the frequency, $\lambda = \frac{2\pi}{k}$ is the wavelength, and the field travels in the x-direction with the phase velocity $V_s = \frac{\omega}{k}$. The sphere is assumed to be small relative to the wavelength of the applied field (that is, $D \ll \lambda$), and to have the permeability of free space.

Since $\frac{D}{\lambda} \ll 1$, the applied field in the vicinity of the sphere may be represented by

$$\bar{B}_a = B_o[\bar{i}_z(j+kx)+\bar{i}_x kz]\, e^{js\omega t} \tag{1}$$

in the reference frame attached to the sphere, where

$$s = \frac{V_s - V_o}{V_s} \tag{2}$$

is the normalized velocity difference between the field and sphere.

The problem is governed by Maxwell's equations with the displacement currents neglected (the usual MHD approximation), and as such requires the solution of the vector diffusion equation within the conductor and Laplace's equation in the surrounding space, subject to four boundary conditions. The usual method for solving problems of this type is to utilize a coordinate system that allows the coordinate surfaces to match the boundaries of the problem and also allows separation of variables in the governing equations. The problem could not be solved by this standard technique as a result of the "conflict" between the two-dimensional nature of the applied field and the three-dimensional nature of the body; hence, an approximate method was developed.

Since the governing equations are linear, the applied field (1) may be thought of as consisting of two parts, a uniform field and a perturbation,

$$\underline{\overline{B}}_a = \underline{\overline{B}}_{ua} + \underline{\overline{B}}_{pa} = \bar{i}_z jB_o + B_o(\bar{i}_z kx + \bar{i}_x kz), \tag{3}$$

where complex notation is used and the $e^{js\omega t}$ is omitted. Then the total magnetic field is represented by (3) plus the induced magnetic field associated with each part of the applied field,

$$\underline{\overline{B}} = \underline{\overline{B}}_a + \underline{\overline{B}}_i = \underline{\overline{B}}_{ua} + \underline{\overline{B}}_{ui} + \underline{\overline{B}}_{pa} + \underline{\overline{B}}_{pi}. \tag{4}$$

If the current density distribution associated with $\underline{\overline{B}}_{ua} + \underline{\overline{B}}_{ui}$ is designated $\underline{\overline{J}}_u$, and that associated with $\underline{\overline{B}}_{pa} + \underline{\overline{B}}_{pi}$ is $\underline{\overline{J}}_p$, then the net time-average force on the sphere is

$$\overline{F} = \frac{1}{2}\mathrm{Re}\left\{\iiint_v \left[\underline{\overline{J}}_u \times \left(\underline{\overline{B}}_{ua}+\underline{\overline{B}}_{ui}\right)^* + \underline{\overline{J}}_p \times \left(\underline{\overline{B}}_{pa}+\underline{\overline{B}}_{pi}\right)^* + \underline{\overline{J}}_u \times \left(\underline{\overline{B}}_{pa}+\underline{\overline{B}}_{pi}\right)^* + \underline{\overline{J}}_p \times \left(\underline{\overline{B}}_{ua}+\underline{\overline{B}}_{ui}\right)^*\right] dv\right\}. \tag{5}$$

For any body that is symmetric with respect to the three major planes through the origin, there can be no net force when either the uniform or the perturbation field alone is applied. As a result, the first two terms in (5) contribute nothing when the integration is carried out. When both the uniform and perturbation fields are applied, the net force arises only from the integral over the terms that couple the two fields.

In the case of a sphere, $\underline{\overline{B}}_{ui}$ and $\underline{\overline{J}}_u$ may be found when $\underline{\overline{B}}_{ua}$ is given, but $\underline{\overline{B}}_{pi}$ and $\underline{\overline{J}}_p$ cannot be found (in practice), given $\underline{\overline{B}}_{pa}$. In short, the net force cannot be determined exactly, but it is reasonable to ask if there are conditions under which the contribution of the $\underline{\overline{J}}_u \times \underline{\overline{B}}_{pa}$ term is large enough to be a reasonable approximation to the exact force. To answer this question, the approximate net force

$$\overline{F}_{upa} = \frac{1}{2} \mathrm{Re}\left\{ \iiint_{v} \underline{\overline{J}_u} \times \underline{\overline{B}^{*}_{pa}} \, dv \right\} \tag{6}$$

is determined for the case of a cylinder and compared with the exact force (5) for that case.

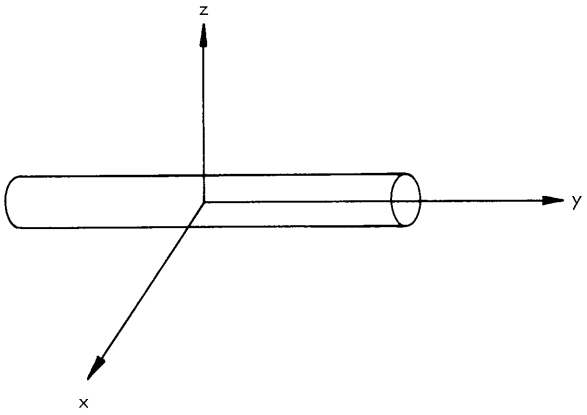

Fig. XIV-6. Orientation of the cylinder.

For the cylinder of infinite length (Fig. XIV-6) the exact time-average force per unit length is calculated and written in dimensionless form as

$$\bar{i}_x \overline{\overline{F}} = \frac{\overline{F}}{\left(\frac{\pi}{4}D^2\right)\left(\frac{B_o^2}{\mu\lambda}\right)} = \bar{i}_x K_{cT}\left(sR_m, \frac{D}{\lambda}\right), \tag{7}$$

where

$$K_{cT} = 2\sqrt{2}\,\pi \frac{b}{U}\left[\frac{a}{b} + \frac{\pi^2}{2}\left(\frac{D}{\lambda}\right)^2\right] \tag{8}$$

$$sR_m = 4U^2 = \mu\sigma s\omega D^2 \tag{9}$$

$$a = \frac{ber_o U(bei_1 U + ber_1 U) + bei_o U(bei_1 U - ber_1 U)}{\left[(ber_o U)^2 + (bei_o U)^2\right]} \tag{10}$$

$$b = \frac{ber_2 U(ber_1 U - bei_1 U) + bei_2 U(bei_1 U + ber_1 U)}{\left[(bei_1 U)^2 + (ber_1 U)^2\right]}, \tag{11}$$

and $ber_\nu U$ and $bei_\nu U$ are Kelvin functions of the first kind of ν. It may be shown that for

$$\frac{\pi^2}{2}\left(\frac{D}{\lambda}\right)^2 \ll 1, \tag{12a}$$

K_{cT} becomes

$$K'_{cT} = 2\sqrt{2}\,\pi\,\frac{a}{U}. \tag{12b}$$

When the approximate force (6) was determined for the cylinder, the result was found to be identical to (12b); hence, the only restriction on the approximate solution is the condition (12a).

Application of this technique to the case of the sphere yields

$$\bar{i}_x\bar{\bar{F}} = \frac{\bar{F}}{\left(\frac{\pi}{6}D^3\right)\left(\frac{B_o^2}{\mu\lambda}\right)} = \bar{i}_x K_s(sR_m), \tag{13}$$

where

$$K_s(sR_m) = \frac{9}{4}\frac{\pi}{u^2}\left\{1 + u\frac{[\tan u(\tanh^2 u - 1) - \tanh u(\tan^2 u + 1)]}{[\tanh^2 u + \tan^2 u]}\right\}, \tag{14}$$

and

$$sR_m = 8u^2 = \mu\sigma s\omega D^2. \tag{15}$$

The "K" functions for the case of the small cylinder (12) and the small sphere (14) are plotted in Figs. XIV-7 and XIV-8, respectively, together with the experimental data.

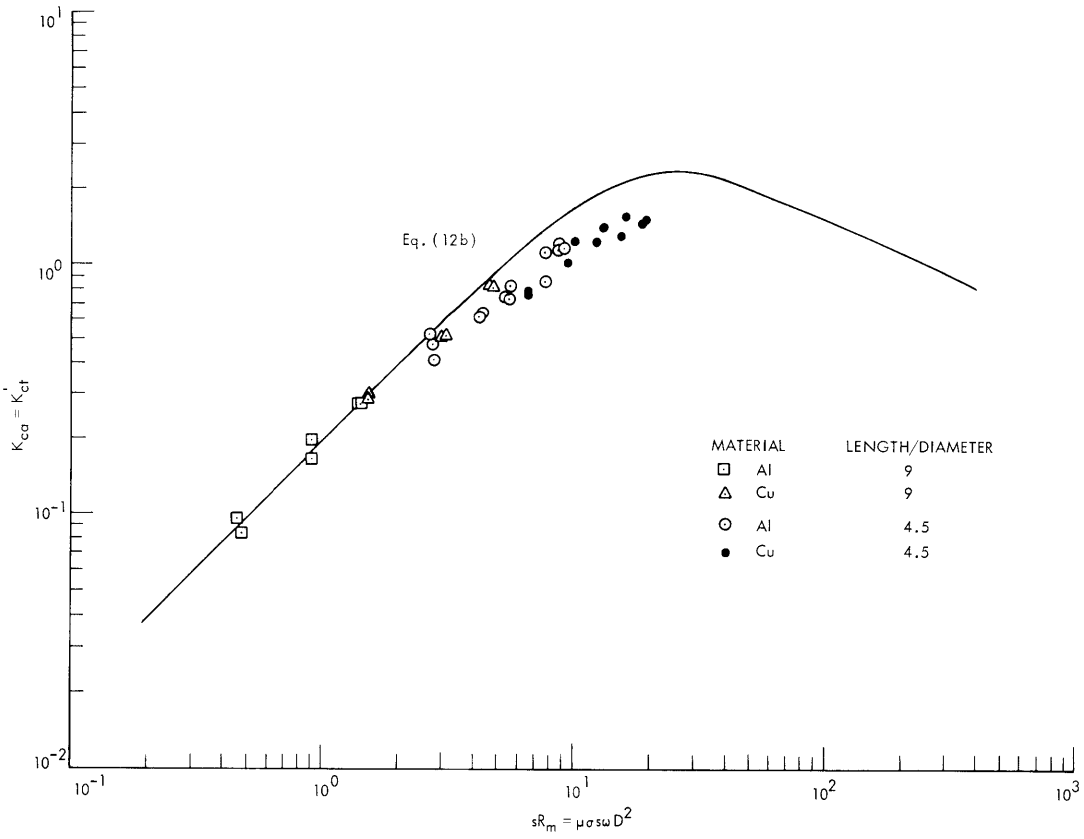

Fig. XIV-7. Correlation of theory with experiment for cylinders such that $\frac{D}{\lambda} \ll 1$.

The latter were obtained by determining the force on a cylinder or sphere suspended in the field produced by the coil system designed by Porter.[1] The characteristics of the conductors used are given in the figures.

In Fig. XIV-7, agreement is quite good over the lower range of sR_m. Departure in

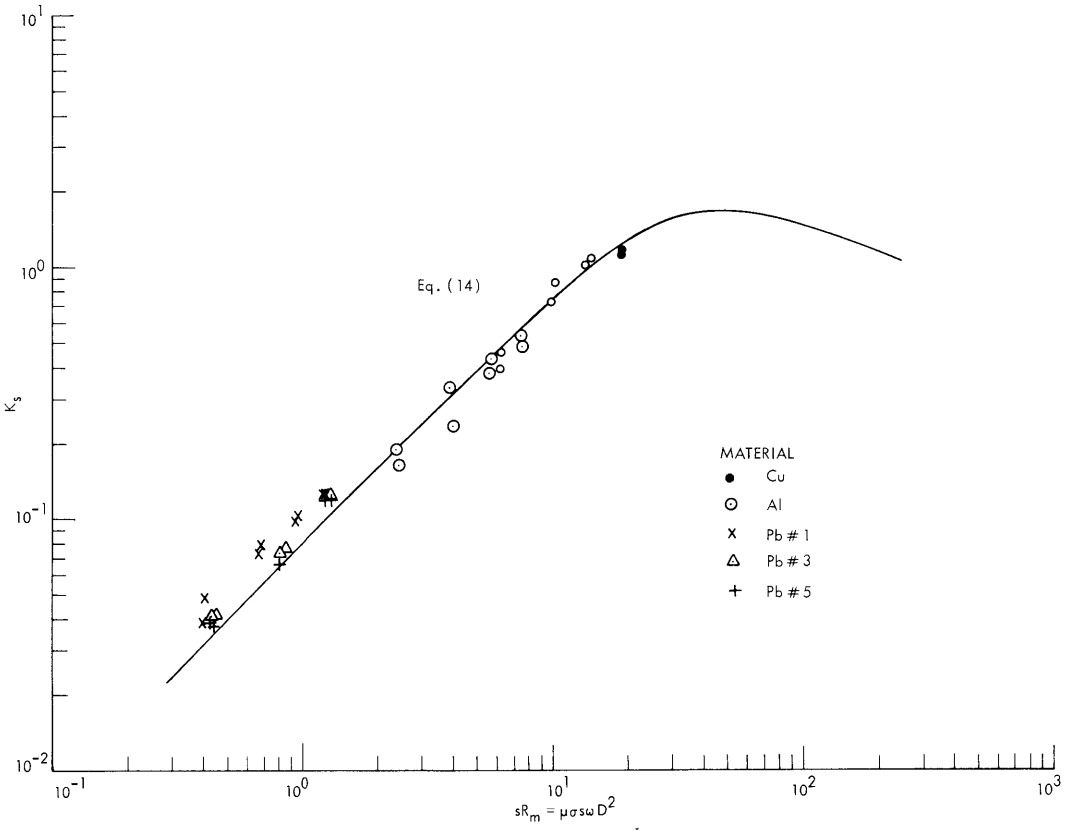

Fig. XIV-8. Correlation of theory with experiment for small spheres. $\frac{D}{\lambda}$; diameter of the test sphere, 1 inch.

the higher range may be attributed to length-to-diameter ratios that were too small to correspond to the two-dimensional model assumed in the solution.

For the sphere, Fig. XIV-8, disagreement is largest at low sR_m, where lead spheres were used. These spheres were cast, so that there was no guarantee of homogeneity, and their surfaces were pockmarked, which would reduce their effective diameter. Experimental error was also largest in this range, since the measured force was smallest.

A solution for the case of the sphere was also obtained by constructing a lumped-parameter model of the sphere and determining the force by the techniques of lumped-parameter electromechanics. This solution appears to converge to (14), so that this technique may be expected to be useful in any similar problem in which the direction,

or approximate direction, of the current density is known at each point in the conductor.

The results above indicate that the single-body interaction is fairly well understood. Therefore, this study will be extended theoretically to cover n noninteracting spheres with a size and velocity distribution, to gain an insight into the characteristics of a mist flow in a traveling magnetic field.

R. J. Thome

References

1. R. P. Porter, "A Coil System for an MHD Induction Generator," S. M. Thesis, Department of Electrical Engineering, M I. T , 1965.

XIV. ENERGY CONVERSION RESEARCH*

B. Alkali-Metal Magnetohydrodynamic Generators

Academic and Research Staff

Prof. J. L. Kerrebrock
Prof. M. A. Hoffman
Prof. G. C. Oates

Graduate Students

R. Decher
M. L. Hougen
D. J. Vasicek
G. W. Zeiders, Jr.

1. STATUS OF RESEARCH: ALKALI-METAL VAPOR MAGNETOHYDRODYNAMIC GENERATORS

During the last quarter a second full-scale run of the large nonequilibrium generator was completed. All components of the facility operated satisfactorily. The test conditions were: stagnation pressure 4.5 atm, stagnation temperature 2000°K, Mach number 2.1, mass-flow rate 0.360 ks^{-1} of He.

The generator was operated at open circuit, and with 3-, 10-, and 25-ohm loads. The open-circuit voltage was between 50 and 70 volts, as compared with ideal values of 500-700 volts at the first and last electrode pairs. When the generator was loaded, the voltage remained nearly constant, while the current per electrode pair increased along the channel, from entrance to exit. For the 3-ohm loads (3 ohms on each electrode pair) the current varied from from 5 amps to ~17 amps. The power for this condition was approximately 5 kilowatts.

This power, while greater than that expected from an equilibrium generator at the same load condition, is much less than that expected from the nonequilibrium generator. It is believed that the low-open-circuit voltage and the resultant low power were due to shorting either in the side-wall boundary layer or in the wall itself. In this generator the wall was made of boron nitrite.

To correct this difficulty, new side walls, of an iron peg-wall construction, have been made. The generator was operated again near the end of May 1966.

During this quarter, the MHD pump for the potassium loop has been rebuilt to provide the higher pressures required for supersonic operation. The supersonic test section is nearly complete. It is expected that the loop will be run during June 1966.

J. L. Kerrebrock

*This work is supported by the U.S. Air Force (Research and Technology Division) under Contract AF33(615)-3489 with the Air Force Aero Propulsion Laboratory, Wright-Patterson Air Force Base, Ohio.

XIV. ENERGY CONVERSION RESEARCH*

C. Hall Instabilities and Their Effect on Magnetohydrodynamic Generators

Academic and Research Staff

Prof. J. E. McCune

Graduate Students

W. H. Evers, Jr.

1. STABILITY CRITERION FOR MAGNETOACOUSTIC WAVES

It has been possible during the past quarter to extend previous work[1] to develop convenient stability criteria for magnetoacoustic waves in the two-temperature conduction regime. It turns out that one can express the stability condition very simply in terms of the convenient parameters

$$Y = \frac{T_{eo}}{T_{go}} - 1$$

$$\delta_{eff}(Y),\ \gamma,\ \frac{E_i}{kT_{go}},$$

where T_{eo} and T_{go} are the DC electron and gas temperatures, E_i is the ionization potential, γ is the ratio of specific heats, and $\delta_{eff}(Y)$ is the "effective collisional loss parameter," including the effect of radiation loss in cooling the electron gas. Various models of the response of the two-temperature ionized gas to magnetoacoustic waves have been assumed, which depend primarily on the rate of ionization relaxation and the effect of radiation "damping" on the waves. In each case the stability criterion can be given in the form

$$\left.\begin{array}{r}\text{unstable if and}\\ \text{only if}\end{array}\right\} \quad \sqrt{\delta_{eff} Y} > \hat{P}\left(Y \left| \frac{E_i}{kT_{go}}, \gamma \right.\right).$$

The form of $\hat{P}(Y)$ depends on which model is assumed. Results are illustrated in Fig. XIV-9 and compared with the experimental data of Dethlefsen.[2]

---

*This work was supported by the U.S. Air Force (Research and Technology Division) under Contract AF33(615)-3489 with the Air Force Aero Propulsion Laboratory, Wright-Patterson Air Force Base, Ohio.

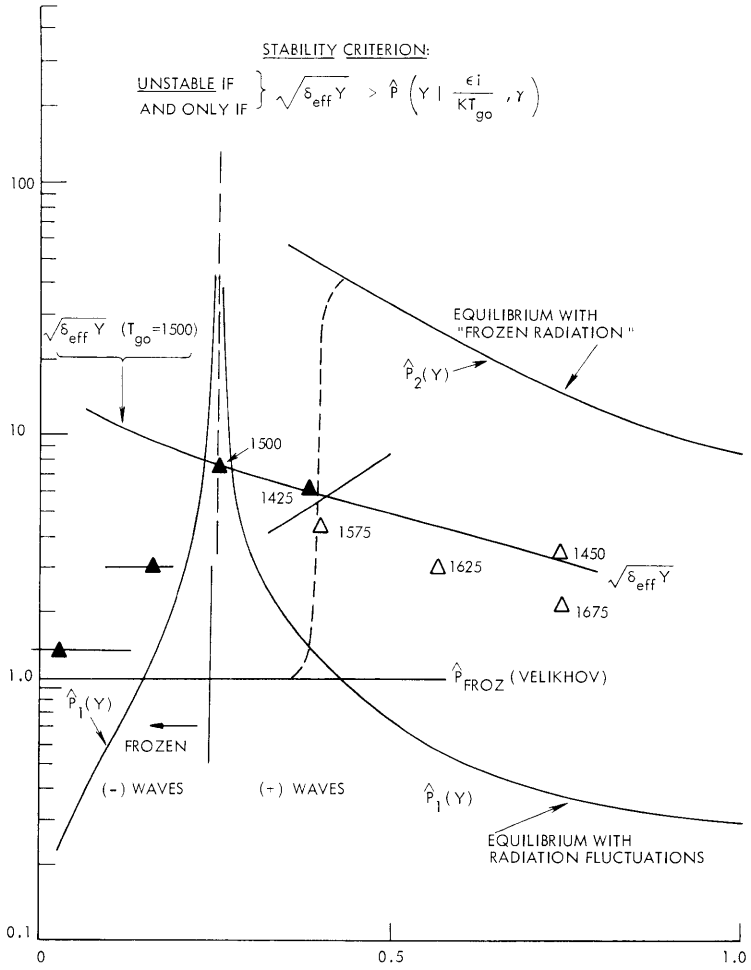

Fig. XIV-9. Stability chart with variables. Dethlefsen's experimental points: Quiet △, Noisy ▲.

Up to a value of Y = 0.4 we expect the ionization to be frozen, in which case $\hat{P} = \hat{P}_{FROZ}$ is simply a constant $= \sqrt{2\gamma/3}$. In this regime the magnetoacoustic waves in Dethlefsen's experimental data should have been unstable; Dethlefsen, in fact, observed strong fluctuations (filled-in points). Above Y = 0.4, the degree of ionization should be in rough equilibrium with the electron gas and we expect one of two models to apply: with the DC state determined largely by radiation loss,[2] either the waves themselves interact strongly with the radiation or they are unaffected by it. The first model leads to $P_1(Y)$ (see Fig. XIV-9), in which case the waves would be strongly unstable. The second model leads to $P_2(Y)$ which shows that they should be stable. Dethlefsen observed a relatively quiet plasma in this regime, which indicated that the waves are not strongly interacting with

the radiation field. This has helped define the need to determine more accurately the nature of the wave-radiation interaction, and work is progressing along these lines, both experimentally and theoretically.

J. E. McCune

References

1. J. V. Hollweg, Master's Thesis, M.I.T., 1965.
2. R. F. Dethlefsen, Ph.D. Thesis, M.I.T., 1965.